Study the Effect of Weight Fractions of Different Powders on the Attenuation Performances of the Epoxy Composite

Khaled W. Yahya[1*], Edrees E. Khadeer[2]

Abstract

Among all types of radiation, X-ray has always garnered the most interest, owing to the growing availability of X-ray tubes in industry, research institutions, and medical facilities. In this research, the linear (μ_l) and mass (μ_m) attenuation coefficient, half value layer (HVL) and mean free path (λ) of the epoxy polymer-based composites which includes both lead oxide (Pb_3O_4), mixture of (Fe_2O_3 + Pb_3O_4) and barium sulfate ($BaSO_4$) with different weight percentages were determined experimentally for the incident photon energies of (29-35 kV) emitted from (X-rays) source. The dispersion of the filler was also investigated using a scanning electron microscope to examine the composites morphology. The obtained results showed that adding these powders to epoxy has an effect on the X-ray shielding abilities of the prepared composites, meaning that there is a direct relationship between the weight ratios of the composite material with the linear (μ_l) and mass (μ_m) attenuation coefficient, and an inverse relationship with the half value layer (HVL) and free path rate (λ). While changing the X-ray shield with applied voltages showed a behavior opposite to what was mentioned above.

The result also shows that the lead oxide (Pb_3O_4) composites yield better attenuation performance than the pure epoxy and the other two composites, especially at high weight fraction (50 Wt.%) of this filler, which due to the high density of these fillers and fine dispensability in the polymer matrix.

Key Words: Epoxy, Radiation Shielding, Polymer Powder Composite, X- ray, Mass Linear attenuation coefficient, Mass Attenuation Coefficient, Half Value Layer, Mean Free Path.

DOI Number: 10.14704/nq.2021.19.9.NQ21147 **NeuroQuantology 2021; 19(9):142-151**

Introduction

X-ray radiation, which is highly ionizing, is extensively utilized in nondestructive testing, medical diagnostics, medical treatment, geological exploration, and security systems. Due to X-ray radiation's biological impacts, its dangers have always garnered more attention. X-rays were recently classified as carcinogenic by the International Committee on Radiological Protection (ICRP) (La, Leatherday, Leong, Watts, & Zhang, 2018; Mirzaei, Zarrebini, Shirani, Shanbeh, & Borhani, 2019). As a result, sheltering X-ray radiation in order to mitigate its carcinogenic and genetic effects, which may result in cell mutations, has become a critical problem in the area of radiological protection (Khoerunnisa et al., 2019; Nambiar & Yeow, 2012).

Shielding for radiation protection is determined by the kind and energy of the radiation. Gamma and X-rays are the most penetrating ionizing radiations. Their interaction is determined by the likelihood of their colliding with the atoms of the materials.

Corresponding author: Khaled W. Yahya
Address: [1*]Department of Physics, College of Science, University of Mosul, Iraq; [2]Department of Physics, College of Science, University of Mosul, Iraq.
E-mail: [1*]khaled.scp93@student.uomosul.edu.iq; [2]dr.adrees@uomosul.edu.iq
Relevant conflicts of interest/financial disclosures: The authors declare that the research was conducted in the absence of any commercial or financial relationships that could be construed as a potential conflict of interest.
Received: 16 July 2021 **Accepted:** 27 August 2021

To enhance the likelihood that they would interact, the density of the material they are traveling through must be raised, which implies that the materials should contain a large number of atoms, with the assumption that the materials are void-free. When working with a porous material, it is necessary to consider the porosity, as it will influence the interactions of the radiations with the atoms inside the material (Noor Azman, 2013).

Due to its high density, high atomic number, and low cost, lead is the most commonly utilized ionizing electromagnetic radiation (IEMR) shielding material. On the other hand, lead has significant drawbacks, including its weight, low mechanical and chemical resistance, rigidity, and toxicity. As a result, its use is restricted, particularly when transportable or wearable shielding materials are required. Nowadays, the demand for new shielding materials is increasing as the applications of IEMR expand due to advancements in technology. To overcome the drawbacks of lead shields, these new shielding materials must be lightweight, non-toxic, and flexible. Composite shielding materials, which combine the characteristics of several materials into a single substance, seem to offer a viable solution to this issue. Polymeric composite materials are one kind of these composite shielding materials. A polymer is utilized as the matrix material and is reinforced with another material. Polymers are utilized for their unique characteristics, which include low density, the ability to create complex forms, optical transparency, cheap production costs, and durability. Whereas larger particles such as metals improve the composites' shielding properties. According to the literature, composite materials composed of polymers and inorganic materials attenuate (IEMR) more than pure polymers but less than pure metals (Abdel-Aziz & Gwaily, 1997; Abdel-Aziz, Badran, Abdel-Hakem, Helaly, & Moustafa, 1991; Abdo, Ali, & Ismail, 2003; Aycik & Belgin, 2018; Hussain, Haq, & Mohammad, 1997; Pavlenko, Lipkanskii, & Yastrebinskii, 2004). In this research, an epoxy resin matrix was filled with three distinct powders to create a composite shielding material for X-rays with energies between 29 and 35 keV. We conducted shielding performance measurements and examined the impact of reinforcing material type of shielding performance.

Experimental Methods

Samples Preparation

Material that is used in preparation of research samples consists of the polymer as a matrix material, low viscosity epoxy (Polyurethan mortar polymer), building industries (22240 INNOPUR FLOOR EPOXY CLEAR COAT) with a density(20˚C) (1.00 ± 0.05 Kg/cm^3). High-pure (99.9% purity) commercial powders of Lead Oxide (30μm, Pb_3O_4) (Hopkin and Williams LTD), Barium Sulphate (45μm, $BaSO_4$) (British Drug Houses LTD) and the mixture of Iron Oxide (Fe_3O_4 + Lead Oxide) (30-50μm) were used for the preparation of composites. `After oven drying, all fillers were sieved to granule size, and the necessary quantity of fillings was produced using an electric balance with an accuracy of (0.001g). Composite samples were prepared by mixing the epoxy resin with five different weight percentages (10, 20, 30, 40 and 50 wt. %) which estimated according to the equation (Crawford, 1987):

$$Wt._P\,\% = \frac{w_p}{w_c} \times 100\% = \frac{w_p}{w_p + w_m} \times 100\% \qquad (1)$$

Epoxy is weighted using electrical balance with sensitivity (10-4 g) for suitable mixing ratio. Powders were added to the epoxy resin and then stirred constantly and gently for (15) minutes in a clean container using a mechanical mixer to achieve reasonably equal dispersion of the powder. Following that, the hardener was gently added to the mixture, stirring constantly to avoid the development of air bubbles inside the sample. The well-mixed mixture was then cast in a plastic rectangular mold having the circle shape with (10mm * 2mm). To complete hardening process, the samples were left for (24) hours at room temperature, followed by heat treatment in the oven at (60 C^o) for (1hr.) to complete the polymerization, the entire assembly was then released and allowed to cure at room temperature for (10) days.

Characterization of Composites

Attenuation Measurements

In order to measure and calculate the attenuation coefficient of the prepared composite samples, a point X-ray source (PHYWE) was used, as shown in figure (1).

Figure 1. X-ray device

The test samples are attached with plastic holder made according to the specifications of the company (phywe) to be suitable to be placed in the stand that moves separately or in combination from the Geiger counter and with an angle relationship between the counter and the sample, as shown in figure (2).

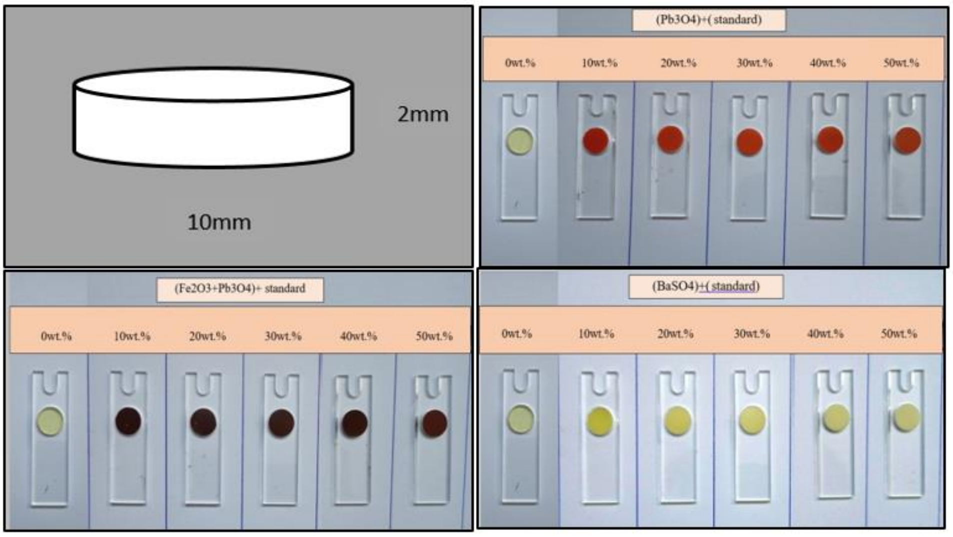

Figure 2. Samples of composite powders

The copper tube of x-ray is fixed in the space allocated to the system, set the specification time in the experiment (100 Sec). The detector angle is then fixed to zero by the Goniometer, the voltage values are determined to the extent that the linear attenuation coefficient of the samples is to be measured, and then measure the intensity of the x-ray falling directly in the absence of samples (I_o) and of X-ray transmission in the presence of samples (I). Steps were repeat by changing voltage values (29, 31, 33, 35 KV).

Linear Attenuation Coefficient Calculations

X-rays interact with the absorber material's atoms, electrons, or nuclei in a variety of ways, and incoming X-rays may be absorbed or dispersed by the material. Thus, after traversing the material, an X-ray beam with an initial intensity of (I_o) of primary photons would have a residual intensity of (I). The linear attenuation coefficient (μ_l) (cm^{-1}) of all prepared specimens was determined using the following relationship (Lilley, 2013):

$$I = I_o \exp^{(-\mu_l x)} \quad (2)$$

$$\mu_l = \frac{\ln\frac{I_o}{I}}{X} \quad (3)$$

In Eq. 3, the parameter (μl) represents the material's total linear attenuation coefficient (cm^{-1}) for X-rays of suitable energy, and (x) represents the material's thickness. We determined the linear attenuation coefficients of composite samples employing X-rays with a range of generation potentials (29 keV-35 keV). Eq. (2) holds true if two criteria are met: To begin, the incident beam's photons are monoenergetic. Second, the beam should be slender (Mheemeed, Hasan, & Al-Jomaily, 2012).

Mass Attenuation Coefficient

The mass attenuation coefficient ((μ_m) (gm/cm^2) is a widely used and useful metric for describing the interaction of radiation with matter. It is measured as the rate of photon interactions inside a unit of mass per 1-unit of area (g/cm^2). It is dependent on the photon's energy and the electrons concentrations in the material It is calculated by dividing (μ_l) by the apparent absorber's density (ρ) (Bashter, 1997).

$$\mu_m = \mu_l \,/\, \rho \quad (4)$$

The apparent density (ρ) of prepared samples was measured using the Archimedes method, which calculated using the equation (N. Z. N. Azman, Siddiqui, & Low, 2013):

$$\rho = \frac{m_1}{m_2 - m_3} \quad (5)$$

Where (m_1), (m_2), and (m_3) are the mass of the sample weighted on the balance, the mass of the sample hanging on balance arm in the air, and the mass of the sample hanging on the balance arm immersed in methanol, whereas (ρ_l) is the density of the immersion methanol liquid.

Half Value Layer Calculations

The term "half-value layer" refers to the thickness of a material at which the intensity of the radiation after it interacts with it is decreased to half that of the photon beam before it enters the material. (HVL), as specified by (Al-Saadi & Saadon, 2017):

$$HVL = 0.693 / \mu_l \quad (6)$$

Where HVL is measured in centimeters (cm) and (μ_l) is the material's linear attenuation coefficient.

Mean of Free Path

The distance that a photon travels through the attenuated medium until it is permanently removed from the beam by absorption interactions (photoelectric effect and pair production) and Compton effect scattering represents the free path rate (λ) for this photon, which can be calculated by the following mathematical relationship (KILIÇ, ERGİN, KARABUL, & ÖZDEMİR, 2019):

$$\lambda = 1 / \mu_l \quad (7)$$

The free path rate is the characteristic of the attenuated medium and the energy of the incident photon.

Results and Discussion

SEM images of epoxy resin reinforced with various weight fractions of ($BaSo4$, Pb_3O_4, Fe_2O_3+Pb_3O_4) powders are presented in figure (2). This method allows the identification of the powders employed and the estimation of their dispersion in the resulting mixes. The microscopy investigations are performed using a scanning electron microscope (ZEISS SIGMA VP).

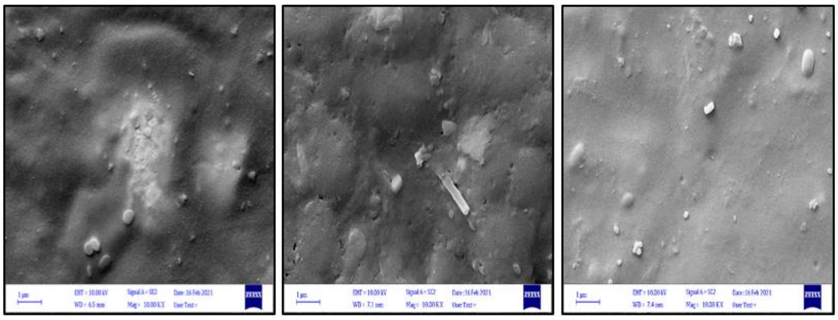

a: Pb_3O_4 b: Pb_3O_4 + Fe_2O_3 c: $BaSo_4$

Figure 3. Microstructure of epoxy reinforced with 10 wt.% of different powders

It can be seen from Figure (3), that there was some extrusion of ($BaSo_4$, Pb_3O_4, Fe_2O_3 + Pb_3O_4) minerals out of epoxy surface, with some of voids as in figures of (a) and (b), which can could be recognized. Surface of samples (b) was wavy appearance and rougher when compared with other samples. This could be due to higher viscosity and prevention of epoxy chains to move freely by (Pb_3O_4 + Fe_2O_3) minerals presented before curing was concluded.

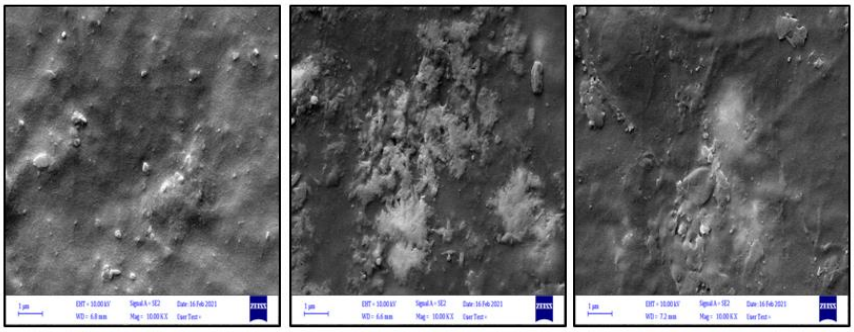

a: Pb_3O_4 b: Pb_3O_4 + Fe_2O_3 c: $BaSo_4$

Figure 4. Microstructure of epoxy reinforced with 50 wt.% of different powders

As shown in figure (4a), after increasing the weight fraction of reinforcing powders, surface of composites seemed to become wavy and rougher. The bright regions represent the filler particles (lead-oxide) dispersed in the dark epoxy matrix. Non-uniform dispersion led to some agglomeration and clusters as can also be seen in figure (4b), and this situation disrupts homogeneity of the (Pb_3O_4 + Fe_2O_3) composite. For a barium sulfate composite, the hazy patches are shown in figure (4c) clearly indicate the presence of certain small filler agglomerations with micro voids. These findings are consistent with those made in the literature (Akgün, 2015).

The figure (4) shows the relationship between the linear attenuation coefficients (μ_l) (whose values were calculated through equation (3) and which directly depends on the values of the transmitted radiation intensity (I)) and both of the applied voltage and the weight ratios of the prepared composite materials (the epoxy and different powders added). The amount of energy of the photons (beam intensity) reaching the sample is in the range (I_o =4874-7381 Count / min).

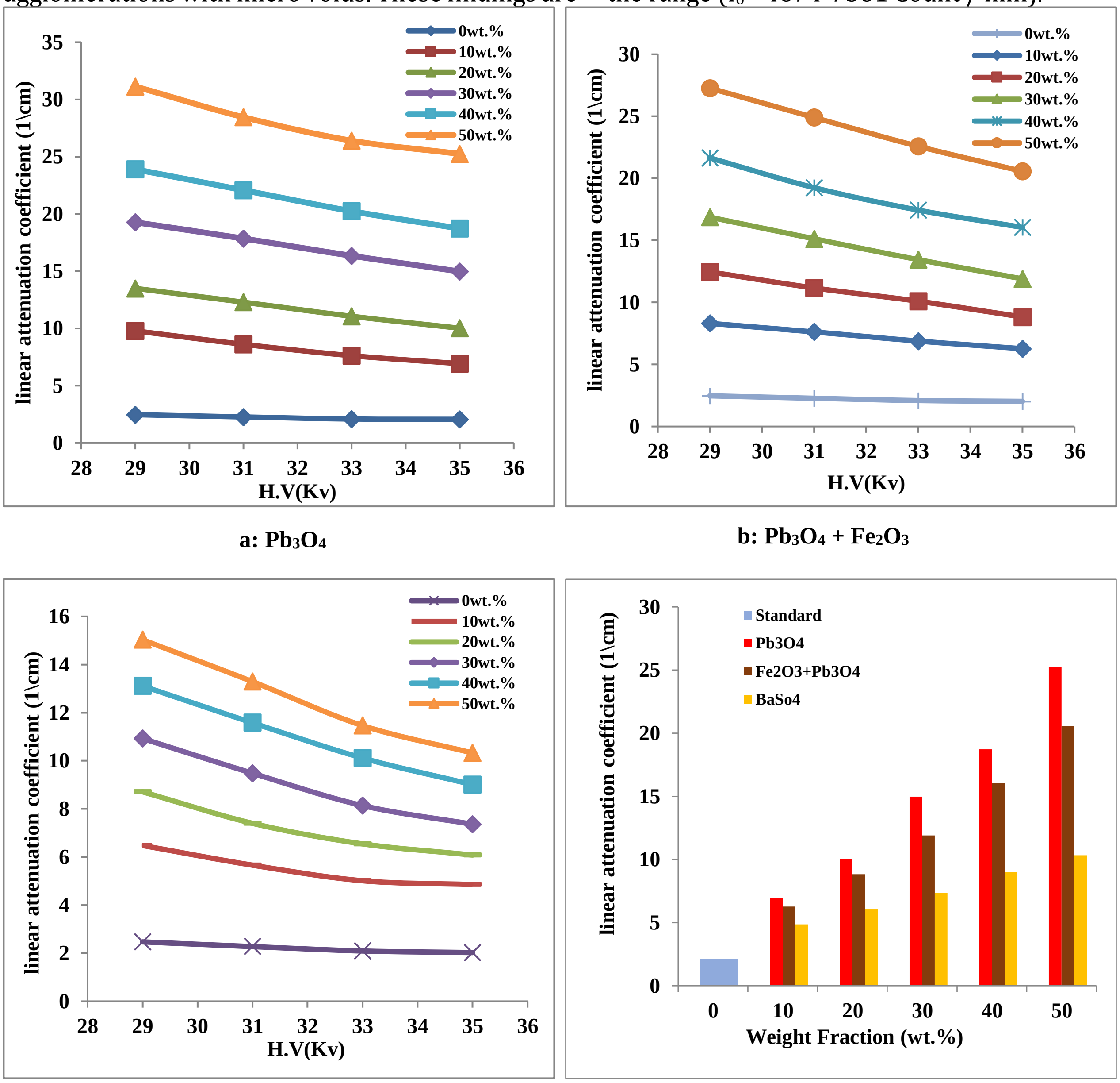

a: Pb_3O_4

b: Pb_3O_4 + Fe_2O_3

c: $BaSo_4$

d: Pb_3O_4, Pb_3O_4 + Fe_2O_3, $BaSo_4$, 35 Kv

Figure 5. Linear attenuation coefficients of powders composites

The results illustrated in figures (5 a, b, c) above shows that, in general, the value of (μ_l) for the fabricated samples were gradually decreased with increasing X-ray applied voltage for all types of testing samples. The average of decreasing values of linear attenuation coefficient for (50 WT.%) (Pb_3O_4)

composite was (19%) from (29-35 Kv), which is the lowest compared to that of the (Fe_2O_3+Pb_3O_4) and ($BaSO_4$), which showed a decrease in the average of decreasing values of the linear attenuation rate of (24%), (31%), respectively, at the same weight fractions and applied voltages.

To know the effect of changing the weighted concentrations of the reinforcing materials on the linear attenuation coefficient rate, see the figure (5d), which take a comparison between attenuation coefficient and weight fractions of reinforcing powders at an applied voltage (35 Kv). We notice an increase in the values of the linear attenuation coefficient when increasing the fractions weight of all types of the reinforcing materials, meaning that there is a direct relationship between the weight ratios of the composite material (the polymer and the addition of powders). The linear attenuation coefficient, and this leads us to the fact that the powder additive increases the surface boundaries of the specimen. Then increases its homogeneity (the presence of strong homogeneity between the polymer and the powder additive) and thus the incident ray beam (I_o) when it is hit by the measurement specimen (polymer and supported by fillers). Then a portion of the photons will be removed from the beam inside the specimen, which leads to a large scattering and attenuation of the photons inside the sample and thus leads to the removal of a portion of the photons permanently. As for the remaining portion of the photons (I), it will be implemented through the sample. From Figure (5d), a value for the linear attenuation coefficient of the pure polymer (without additives) was obtained to compare it with the remaining ratios when adding different types of powder to the polymer to see the usefulness of the addition. Whether or not, and what is the composite material that showed the highest rate of X-ray attenuation.

The value of the linear attenuation coefficient of the pure polymer is (2.0684 cm^{-1}). The highest value of the linear attenuation coefficient was obtained for the lead oxide (Pb_3O_4) composite, which is (25.2543 cm^{-1}) at the weight fraction, which is (50 wt.%), and the lowest value was noticed (Fe_2O_3+Pb_3O_4) and ($BaSO_4$) composite, at the same weight fraction, which is (20.5687 cm^{-1}) and (10.3252 cm^{-1}), respectively. This lead to conclude that the (Pb_3O_4) composite give better attenuation against X-ray photons than the other two fillers (Fe_2O_3+Pb_3O_4) and ($BaSO_4$) composite.

The deficiency in the performance of the last two composites can be attributed to the heterogeneity in the distribution of the support powders in the base material which led to some agglomeration and clusters of reinforcing powders, that was previously shown by microscopic imaging, which does not cover all sides and sides of the sample (i.e. not filling all the spaces between the polymeric chains) and this leads to the presence of residual spaces between the polymer parts that allow the bulk of the radiation to pass through this sample.

The mass attenuation coefficient enables straightforward comparisons of the radiation shielding effectiveness of various shielding materials. Fig. 6 illustrates the mass attenuation coefficient, (μ_m), as a function of X-ray tube voltage and the weight percent of various fillers in composites at (35 Kv) X-ray energy for pure epoxy and reinforced samples.

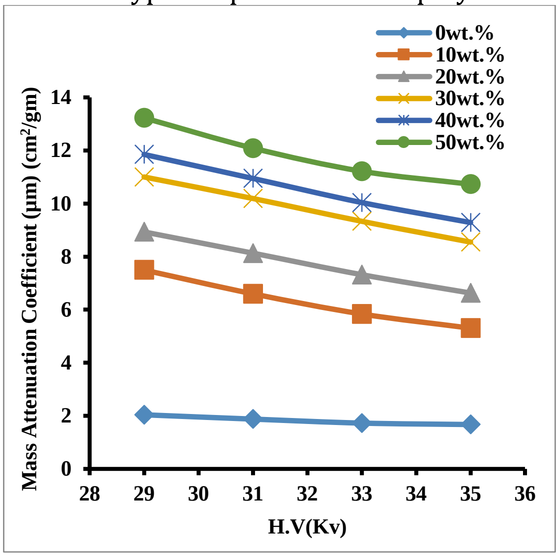

a: Pb_3O_4

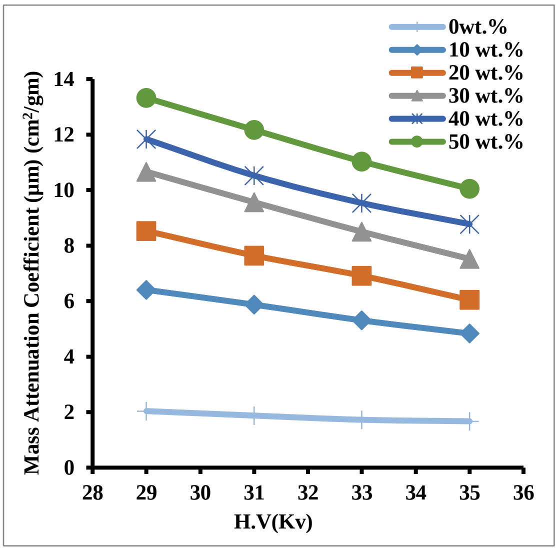

b: Pb_3O_4 + Fe_2O_3

eISSN 1303-5150

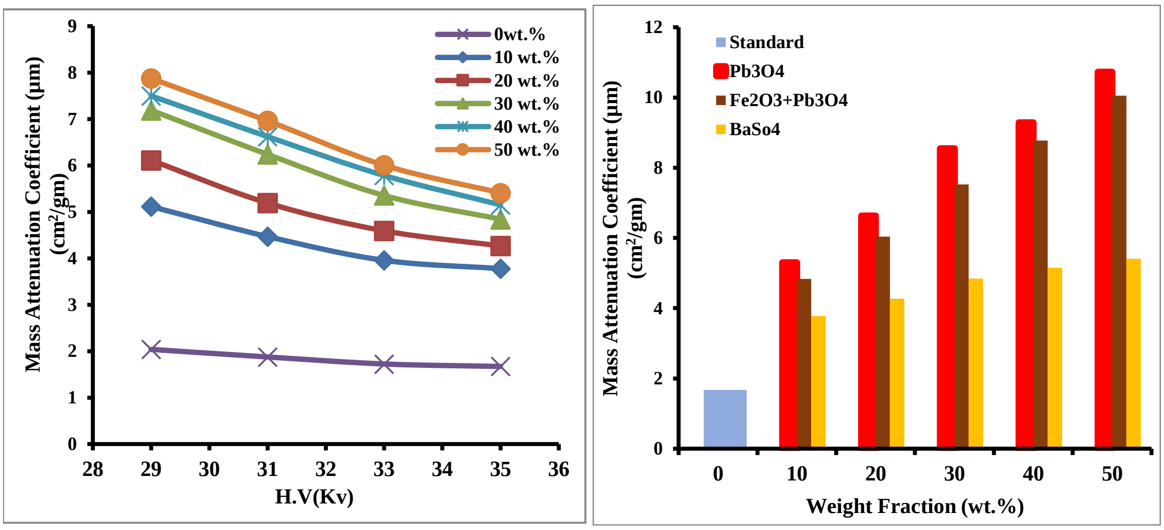

c: BaSo4 **d: Pb_3O_4, Pb_3O_4 + Fe_2O_3, $BaSO_4$, 35 Kv**

Figure 6. Mass attenuation coefficients of powders composites

As shown in figures (6a, b, c), for all kinds of pure and manufactured composites, there is a typical reduction in (μ_m) as the X-ray tube excitation voltage increases. The average of decreasing values of mass attenuation coefficient for (50 WT.%) (Pb_3O_4) composite was (19%) from (29-35 Kv), which is the lowest compared to that of the (Fe_2O_3+Pb_3O_4) and ($BaSO_4$), which showed a decrease in the average of decreasing values of the linear attenuation rate of (25%), (31%), respectively, at the same weight fractions and applied voltage. The high (μ_m) coefficient for lower photon energies is attributed to the high possibility of occurrence of photon absorption via photoelectric effect, which is directly proportional to the (Z). Only in photoelectric absorption, the incident x-ray photons which interact is completely absorbed and as many photons are straight away removed from the incident flux (Harish, Nagaiah, & Kumar, 2012; Li et al., 2017). In other hand, the mass attenuation coefficients of (Pb_3O_4) composite are higher than that of (Pb_3O_4+Fe_2O_3), ($BaSO_4$) composites and the base material, for example, the mass attenuation coefficients is equal (10.7278 cm²/gm) for (Pb_3O_4) and (10.0477 cm²/gm), (5.4087 cm²/gm) and (1.6715 cm²/gm) for (50 wt.%) (Fe_2O_3+Pb_3O_4), ($BaSO_4$) and pure polymer, respectively.

For (This indicates that the (Pb_3O_4) composite absorbs more photons than the other composites stated before, which had lower transmittances for the same filler content (sample thickness was (2 mm), and photon energy of X-rays was (35 keV)), as shown in figure (6 d). This rise in mass attenuation coefficient for (Pb_3O_4) in contrast to other kinds of composites may be ascribed to increased concentrations of (Pb), which has a greater atomic number than other elements.

The variance in the mass attenuation coefficients of the prepared composites is a result of the difference in densities between those composites, which is an inevitable result of increasing the weight concentrations of the added reinforcement materials compared to the unsupported base material (KILIÇ et al., 2019), as shown in Table (1). As well as, the defects that appeared in the composites after the casting process, which were seen in the microscopy, also played a role in the difference in the observed mass attenuation coefficients.

Table 1. Chemical composition and density of epoxy composites

	(pb_3O_4)	(Fe_2O_3+Pb_3O_4)	($BaSO_4$)
Wt.%	**ρ(gm/cm³)**	**ρ(gm/cm³)**	**ρ(gm/cm³)**
0	**1.21209**	**1.21209**	**1.21209**
10	**1.3063**	**1.2976**	**1.2664**
20	**1.5122**	**1.4608**	**1.4252**
30	**1.7523**	**1.58218**	**1.5197**
40	**2.0170**	**1.8291**	**1.7484**
50	**2.3541**	**2.0471**	**1.909**

This lead to conclude that the (Pb_3O_4) composite give better attenuation against X-ray photons than the other two fillers (Fe_2O_3+Pb_3O4) and ($BaSO_4$) composite. The deficiency in the performance of the last two composites can be attributed to the heterogeneity in the distribution of the support powders in the base material which led to some agglomeration and clusters of reinforcing powders, that was previously shown by microscopic imaging, which does not cover all sides and sides of the sample (i.e. not filling all the spaces between the polymeric chains) and this leads to the presence of residual spaces between the polymer parts that allow the bulk of the radiation to pass through this sample to determine the photon absorption ability of a radiation shielding material, along with the mass attenuation coefficient, the critical thicknesses of half value layer (HVL) and mean free path (λ) are commonly used. The reinforcing material weight and voltage dependencies of (HVL) were shown in Figure (7) for the epoxy composites including (Pb_3O_4), (Fe_2O_3+Pb_3O_4) and ($BaSO_4$) with different wt. Percentages at the incident photon energies rang varying from (29-35 Kv).

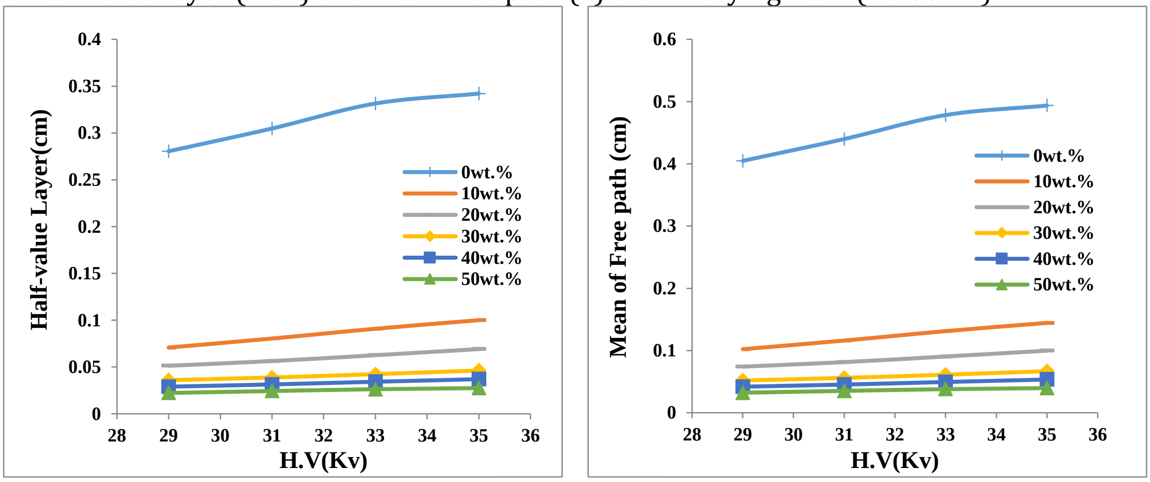

a: Pb_3O_4

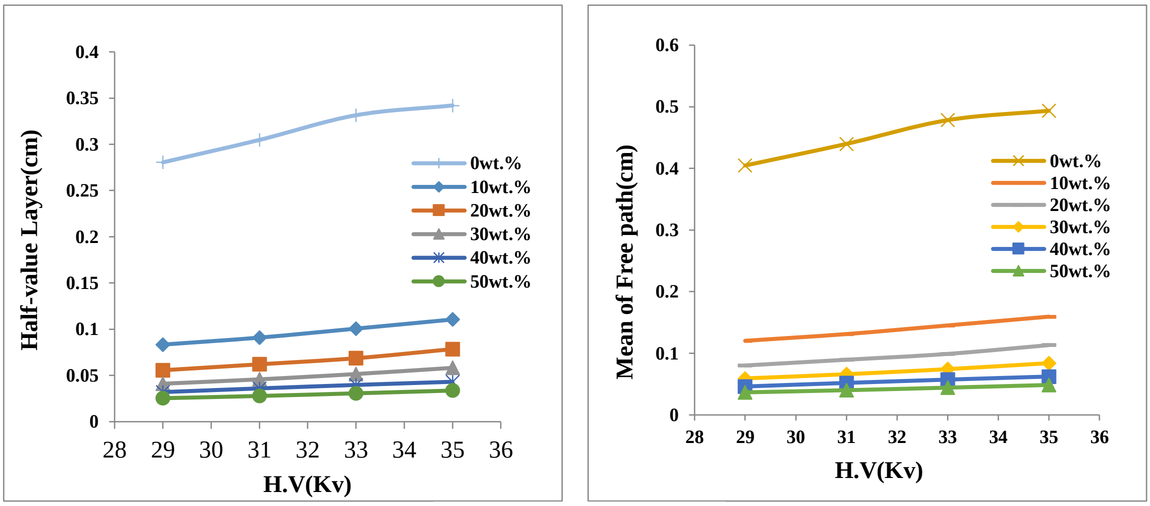

b: Pb_3O_4 + Fe_2O_3

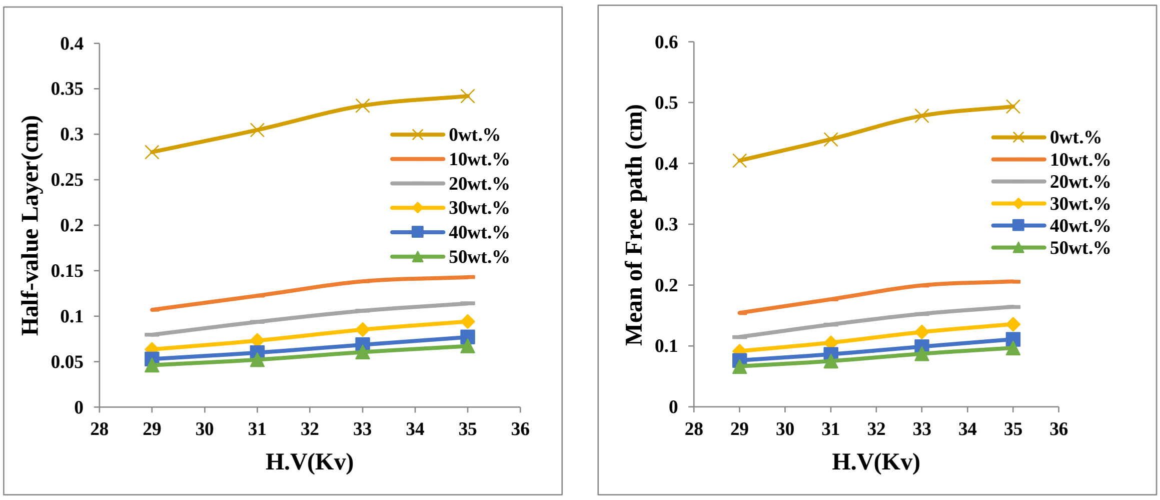

c: $BaSo_4$

Figure 7. The half value layer and the mean of free path of powders composites

*e*ISSN 1303-5150

It is noted from the figures that the values of the half-thickness (HVL) increase with the increase in the applied voltage. This is explained on the basis that high energies need a layer of thickness half greater in order to attenuate it to half its original value than low energies need and this is consistent with the study (Akgün, 2015). It was also found that the (Pb_3O_4) composite gives lower (HVL) at all voltages than (Fe_2O_3 + Pb_3O_4), ($BaSO_4$) and pure epoxy, as shown in table (2), this can be attributed to increasing values of (Pb), which has a higher atomic number than the other elements, indicating the benefit of lead in radiation shielding composites (Al-Saadi & Saadon, 2017; N. N. Azman, Siddiqui, Ionescu, & Low, 2012). The homogeneity of the samples for the filler powders can also play an important role in obtaining these results. A good distribution of the reinforcing powder leads to reduce the percentages of radiation penetration.

Figure (7) also shows the relationship between (λ) (whose value was calculated through equation (5) and which directly depends on the values of the linear attenuation coefficient (μ)) with the applied voltage and weight ratios of the composite material. We conclude that there is increase of (λ) with increasing of the applied voltage, and a decrease with increasing the weight ratios for all types of reinforcement additions, especially for (Pb_3O_4) composite which gives a lower free path rate than (Fe_2O_3+Pb_3O_4), ($BaSO_4$) and pure epoxy at all voltages. Because the values of (λ) depend entirely on the values of the linear attenuation, which has an inverse relationship between them, as shown in table (2), at the applied voltage (35 Kv), and this is consistent with the study (Shaymaa, 2018).

Table 2. The value of (HVL) and (λ) of epoxy composites at photon energy 35 Kv

wt.%	Pb_3O_4			Fe_2O_3+Pb_3O_4			$BaSo_4$		
	μ_l	HVL	λ	μ_l	HVL	λ	μ_l	HVL	λ
0	2.02601	0.342050	0.49357	2.02601	0.342050	0.49357	2.02601	0.342050	0.49357
10	6.92869	0.100018	0.14432	6.52493	0.106207	0.15325	4.85302	0.142797	0.20605
20	10.02196	0.069148	0.09978	9.47688	0.073125	0.10551	6.08173	0.113947	0.16442
30	14.97628	0.046273	0.06677	11.8994	0.058238	0.08403	7.35966	0.094161	0.13587
40	18.7274	0.037004	0.05339	16.04908	0.043180	0.0623	9.00833	0.076928	0.111
50	25.25433	0.027440	0.03959	20.56871	0.033691	0.04861	10.32526	0.067116	0.09684

Conclusions

1. The study demonstrated that selecting materials for X-ray shielding requires an understanding of a number of parameters, including the linear and mass attenuation coefficients (μ_l, μ_m), the half-thickness (HVL), and the free path (λ), which are all dependent on the energy of the incident photon, the weight fraction, density, and chemical composition of the prepared composite materials.
2. The results showed that the values of the attenuation coefficients for (X-rays) are inversely proportional to the operating voltages of X-rays and directly to the weight fractions of the reinforcement materials. While both (HVL) and (λ) showed the opposite behavior to what was mentioned above.
3. It is also clear that the lead oxide (Pb_3O_4) composite has the highest value of the linear and mass attenuation coefficients and lower value of the half-thickness and the free path rates of the X-ray photon than (Fe_2O_3 + Pb_3O_4) and ($BaSO_4$), composites, at all weight fractions of the fillers and the applied voltages.

References

Abdel-Aziz M, Gwaily S. Thermal and mechanical properties of styrene-butadiene rubber/lead oxide composites as gamma-radiation shields. *Polymer degradation and stability* 1997; 55(3): 269-274.

Abdel-Aziz M, Badran A, Abdel-Hakem A, Helaly F, Moustafa A. Styrene–butadiene rubber/lead oxide composites as gamma radiation shields. *Journal of applied polymer science* 1991; 42(4): 1073-1080.

Abdo AES, Ali M, Ismail M. Natural fibre high-density polyethylene and lead oxide composites for radiation shielding. *Radiation Physics and Chemistry* 2003; 66(3): 185-195.

Akgün AM. *Reinforcement of polyesters by boron minerals.* A Thesis Submitted to the Graduate School of Natural and Applied Sciences of Middle East Technical University 2015. http://etd.lib.metu.edu.tr/upload/12619368/index.pdf

Al-Saadi AJ, Saadon AK. Gamma Ray Attenuation Coefficients for Lead Oxide and Iron Oxide Reinforced in Silicate Glasses as Radiation Shielding Windows. *Ibn AL-Haitham Journal for Pure and Applied Science* 2017; 27(3): 201-214.

Aycik G, Belgin EE. Effect of polymer matrix type on electromagnetic radiation shielding performances of PbO reinforced/polyethylene, isophytalic polyester and bisphenol A vinylester based composites. *International Journal of Chemistry and Chemical Engineering Systems* 2018, *3*.

Azman NN, Siddiqui S, Ionescu M, Low I. Synthesis and characterisation of ion-implanted epoxy composites for

X-ray shielding. *Nuclear Instruments and Methods in Physics Research Section B: Beam Interactions with Materials and Atoms* 2012; 287: 120-123.

Azman NZN, Siddiqui SA, Low IM. Synthesis and characterization of epoxy composites filled with Pb, Bi or W compound for shielding of diagnostic x-rays. *Applied Physics A* 2013; 110(1): 137-144.

Bashter I. Calculation of radiation attenuation coefficients for shielding concretes. *Annals of nuclear Energy* 1997; 24(17): 1389-1401.

Crawford RJ. *Plastic Engineering*. U.K: Pergamon Press 1987.

Harish V, Nagaiah N, Kumar HG. Lead oxides filled isophthalic resin polymer composites for gamma radiation shielding applications. *Indian Journal of Pure & Applied Physics (IJPAP)* 2012; 50(11): 847-850.

Hussain R, Haq ZU, Mohammad D. A study of the shielding properties of poly ethylene glycol-lead oxide composite. *Journal of Islamic Academy of Sciences* 1997; 10(3): 81-84.

Khoerunnisa F, Futamura R, Mukai S, Konishi T, Fujikawa T, Kaneko K. X-ray absorption anomaly of well-characterized multiwall carbon nanotubes. *Carbon* 2019; 145: 209-217.

Kiliç M, Ergin Y, Karabul Y, Özdemir ZG. Experimental Comparison of PbO and BaO Addition Effect on Gamma Ray Shielding Performance of Epoxy Polymer. *Avrupa Bilim ve Teknoloji Dergisi* 2019; (16): 256-266.

La LB, Leatherday C, Leong YK, Watts HP, Zhang LC. Green lightweight lead-free Gd2O3/epoxy nanocomposites with outstanding X-ray attenuation performance. *Composites Science and Technology* 2018; 163: 89-95.

Li R, Gu Y, Zhang G, Yang Z, Li M, Zhang Z. Radiation shielding property of structural polymer composite: continuous basalt fiber reinforced epoxy matrix composite containing erbium oxide. *Composites Science and Technology* 2017; 143: 67-74.

Lilley J. *Nuclear physics: principles and applications*: John Wiley & Sons 2013.

Mheemeed A, Hasan H, Al-Jomaily F. Gamma-ray absorption using rubber—lead mixtures as radiation protection shields. *Journal of Radioanalytical and Nuclear Chemistry* 2012; 291(3): 653-659.

Mirzaei M, Zarrebini M, Shirani A, Shanbeh M, Borhani S. X-ray shielding behavior of garment woven with melt-spun polypropylene monofilament. *Powder Technology* 2019; 345: 15-25.

Nambiar S, Yeow JT. Polymer-composite materials for radiation protection. *ACS applied materials & interfaces* 2012; 4(11): 5717-5726.

Noor Azman NZB. *Design of nanostructured polymeric materials for radiation shielding of ionizing radiations.* Curtin University 2013.

Pavlenko V, Lipkanskii V, Yastrebinskii P. Calculations of the passage of gamma-quanta through a polymer radiation-protective composite. *Journal of Engineering Physics and Thermophysics* 2004; 77(1): 11-14.

Shaymaa SH. Measurement and study linear attenuation coefficient of x-ray for epoxy/titanium oxide composites. *Journal of Wassit For Science & Medicine* 2018; 11(1), 172-182.

Pandarakalam JP. The physiology of incarnation process; lessons from pre-birth experiences and reincarnation-type case. *NeuroQuantology* 2019; 17(5): 22-34.

*e*ISSN 1303-5150